Dynamical consequences of adaptation of the growth rates in a system of three competing populations

2001 J. Phys. A: Math. Gen. 34 7459

(http://iopscience.iop.org/0305-4470/34/37/303)

INSTITUTE OF PHYSICS PUBLISHING JOURNAL OF PHYSICS A: MATHEMATICAL AND GENERAL

J. Phys. A: Math. Gen. **34** (2001) 7459–7473 PII: S0305-4470(01)21595-9

Dynamical consequences of adaptation of the growth rates in a system of three competing populations

Zlatinka I Dimitrova[1,2] **and Nikolay K Vitanov**[1,3]

[1] Max-Planck Institute for Physics of Complex Systems, Noethnitzerstrasse 38, 01187 Dresden, Germany
[2] Institute of Solid State Physics, Bulgarian Academy of Sciences, Blvd Tzarigradsko Chaussee 72, 1784 Sofia, Bulgaria

E-mail: vitanov@mpipks-dresden.mpg.de

Received 30 January 2001, in final form 12 June 2001
Published 7 September 2001
Online at stacks.iop.org/JPhysA/34/7459

Abstract

We investigate the nonlinear dynamics of a system of populations competing for the same limited resource for the case where each of the populations adapts its growth rate to the total number of individuals in all populations. We consider regions of parameter space where chaotic motion of the Shilnikov kind exists and present results for two characteristic values of the growth ratio adaptation factor r^*: $r^* = -0.15$ and 5. Negative r^* can lead to vanishing of regions of chaotic motion and to a stabilization of a fixed point of the studied model system of differential equations. Positive r^* lead to changes of the shape of the bifurcation diagrams in comparison with the bifurcation diagrams for the case without adaptation. For the case $r^* = 5$ we observe transition to chaos by period-doubling bifurcations, windows of periodic motion between the regions of chaotic motion and a region of transient chaos after the last window of periodic motion. The Lyapunov dimension for the chaotic attractors is close to two and the Lyapunov spectrum has a structure which allows a topological analysis of the attractors of the investigated system.

PACS numbers: 05.45.Ac, 05.45.-a, 87.23.Cc

1. Introduction

The mathematical modelling of systems of competing populations leads to understanding of the characteristics of the process of evolution. The properties of the obtained equations are very interesting from the point of view of the nonlinear dynamics [1–11]. Many of the mathematical models of the population dynamics are based on the Lotka–Volterra equations [12–21]. In this

[3] To whom correspondence should be addressed.

paper we discuss an extension of the model of competing populations based on the generalized Volterra equations

$$\frac{\mathrm{d}N_i\,(t)}{\mathrm{d}t} = r_i N_i(t)\left[1 - \sum_{j=1}^{n} \alpha_{ij} N_j(t)\right] \qquad i = 1, 2, \ldots, n \tag{1}$$

where r_i is the growth rate of the ith population, and the competition coefficients α_{ij} characterize to what extent the jth species affects the growth rate of the ith species. Finally N_i is the number of individuals of the ith population. If we set the competition coefficients α_{ij} to zero we obtain a system of equations that describes a process of exponential growth. As the number of individuals of the populations must be finite the Volterra equations contain terms that describe the competition among the populations for the limited natural resources. Thus the growth terms are compensated by the competition terms.

In the model (1) the growth rates and competition coefficients do not change. In the natural systems we observe the phenomenon of adaptation. Our idea is to include this phenomenon in the above-mentioned mathematical model and to investigate its dynamical consequences. In [22] we have assumed that the competition coefficients and growth rates in the generalized Volterra equations depend on the number of individuals of the populations in the following way:

$$r_i = r_i^0\left[1 + \sum_{k=1}^{n} r_{ik} N_k\right] \qquad \alpha_{ij} = \alpha_{ij}^0\left[1 + \sum_{k=1}^{n} \alpha_{ijk} N_k\right]. \tag{2}$$

r_{ik} and α_{ijk} are the growth rate adaptation factors and competition coefficient adaptation factors of first order. Thus we obtain the classical model as a particular case when the adaptation factors are zero. Moreover (2) is the simplest way to take into account the adaptation of the growth rates and competition coefficients and to avoid an explicit introduction of a dependence on the time. Substituting (2) into (1) we obtain

$$\frac{\mathrm{d}N_i}{\mathrm{d}t} = r_i^0 N_i\left\{1 - \sum_{j=1}^{n}[\alpha_{ij}^0 - r_{ij}]N_j - \sum_{j=1}^{n}\sum_{l=1}^{n} \alpha_{ij}^0[\alpha_{ijl} + r_{il}]N_j N_l - \sum_{j=1}^{n}\sum_{k=1}^{n}\sum_{l=1}^{n} \alpha_{ij}^0 r_{ik}\alpha_{ijl} N_j N_k N_l\right\}. \tag{3}$$

Equation (3) leads to many possibilities. For an example it contains as particular cases the model of Gilpin [23, 24] and the model of low-dimensional replicator systems [25]. If r_i^0 and α_{ij}^0 are functions of $N_{1,2,3}$ then (3) contains as a particular case the Hastings–Powell model [26, 27]. In this paper we shall discuss the competition and adaptation for the case

$$r_{ik} = r^* \qquad \alpha_{ijk} = \alpha^* \tag{4}$$

corresponding to populations of different subkinds of the same kind of animal. We can easily see that (4) leads to adaptation of each population with respect to the total number of individuals of all populations. Introducing the parameters

$$r_i^0 = \sum_{j=1}^{n} \kappa_{ij} \qquad r_i^0 \alpha_{ij}^0 = \kappa_{ij} \tag{5}$$

and taking into account (4), equation (3) is reduced to the system discussed in [28] plus additional terms A_i due to the adaptation effects

$$\frac{\mathrm{d}N_i}{\mathrm{d}t} = N_i \sum_{j=1}^{n} \kappa_{ij}(1 - N_j) + A_i \tag{6}$$

$$A_i = r_i^0 N_i\left\{r^* \sum_{j=1}^{n} N_j - (\alpha^* + r^*) \sum_{j,l=1}^{n} \alpha_{ij}^0 N_j N_l - \alpha^* r^* \sum_{j,k,l=1}^{n} \alpha_{ij}^0 N_j N_k N_l\right\}. \tag{7}$$

κ_{ij} is

$$\kappa_{ij} = \begin{pmatrix} \kappa_1 & \kappa_1 & \kappa_2 \\ -\kappa_1 & -\kappa_2 & \kappa_2 \\ \kappa_3 & \kappa_2 & \kappa_2 \end{pmatrix}.$$

When $\kappa_1 = 0.5$, $\kappa_2 = 0.1$ and $\kappa_3 = \mu$ we obtain as a particular case the case discussed in [22]. If in addition $\alpha^* = r^* = 0$ we obtain the case discussed in [28]. For the most cases discussed in this paper we shall fix $\kappa_3 = 1.43$ and change κ_1 and κ_2 in order to investigate the regions of parameter space where the dynamics of the numbers of the population individuals satisfies the theorem of Shilnikov [29–31]. In addition we set $\alpha^* = 0$; $r^* \neq 0$, i.e. we shall investigate the influence of the adaptation of the growth rates of the populations on the system dynamics.

This paper is organized as follows. In the following section we discuss the intervals of the system parameters where two of the fixed points of (6) satisfy the theorem of Shilnikov and the stability of these fixed points. In section 3 we discuss the system dynamics in the above-mentioned regions of the parameters and analyse the power spectra, histograms and autocorrelations. In section 4 we calculate the Lyapunov spectrum and the Lyapunov dimension. Finally we show that the dissipativity of the system increases with increasing growth ratio adaptation factor r^*.

2. Area of applicability of the theorem of Shilnikov

When the parameter $\kappa_3 = 1.43$ and for the case without adaptation ($\alpha^* = r^* = 0$) the system (6) possesses a strange attractor [28]. It is a consequence of a theorem of Shilnikov which states that if for the system

$$\frac{\mathrm{d}x}{\mathrm{d}t} = \rho x - \omega y + P(x, y, z) \tag{8a}$$

$$\frac{\mathrm{d}y}{\mathrm{d}t} = \omega x + \rho y + Q(x, y, z) \tag{8b}$$

$$\frac{\mathrm{d}z}{\mathrm{d}t} = \lambda z + R(x, y, z) \tag{8c}$$

(P, Q, R are C^r functions ($1 \leqslant r \leqslant \infty$) vanishing together with their first derivative at $O = (0, 0, 0)$) then an unstable orbit Γ exists, which is a homoclinic connection, and if

$$\lambda > -\rho > 0 \tag{9}$$

then every neighbourhood of the orbit Γ contains a denumerable set of unstable periodic solutions of saddle type.

Chaotic motion can be obtained by means of the above theorem if two appropriate fixed points $P_{1,2}$ exist. The first of them must be a saddle focus and has to satisfy the condition (9) in some region of the space of the system parameters. The second point P_2 must undergo a supercritical Hopf bifurcation in this region of parameters. When $\alpha^* = 0$ and $r^* \neq 0$ we obtain the same fixed points as in the case $\alpha^* = r^* = 0$ plus the additional fixed points ($N_1 = -(1 + r^* N_2)/r^*$, N_2: arbitrary, $N_3 = 0$) and ($N_{1,3}$: arbitrary, $N_2 = -(1 = r^* N_3 + r^* N_1)/r^*$). Thus the saddle focus P_1 and the point P_2, where a Hopf bifurcation occurs, are the same as the corresponding points for the case without adaptation. The coordinates of the saddle focus are

$$N_1 = \frac{-2\kappa_2\kappa_1 + \kappa_1^2 - \kappa_2^2}{\kappa_1(-\kappa_2 + \kappa_1)} \qquad N_2 = \frac{\kappa_1 + \kappa_2}{-\kappa_2 + \kappa_1} \qquad N_3 = 0. \tag{10}$$

The coordinates of the fixed point P_2 where the Hopf bifurcation arises are $N_{1,2,3} = 1$. The adaptation of the growth rates does not influence the positions of the points $P_{1,2}$ but it influences their stability. The eigenvalues connected to the linear stability of the saddle focus P_1 are

$$\lambda_1 = (\kappa_1 + 2r^*\kappa_1 + r^*\kappa_2)\Big[-\kappa_1^2 + 3\kappa_1\kappa_2 + 2\kappa_2^2 + \sqrt{-3\kappa_1^4 + 2\kappa_1^3\kappa_2 + 13\kappa_1^2\kappa_2^2 + 4\kappa_1\kappa_2^3}\Big]\Big/(2\kappa_1(\kappa_1 - \kappa_2)) \tag{11a}$$

$$\lambda_2 = (\kappa_1 + 2r^*\kappa_1 + r^*\kappa_2)\Big[-\kappa_1^2 + 3\kappa_1\kappa_2 + 2\kappa_2^2 - \sqrt{-3\kappa_1^4 + 2\kappa_1^3\kappa_2 + 13\kappa_1^2\kappa_2^2 + 4\kappa_1\kappa_2^3}\Big]\Big/(2\kappa_1(\kappa_1 - \kappa_2)) \tag{11b}$$

$$\lambda_3 = \kappa_2\big[2\kappa_1^3 r^* + 2r^*\kappa_1^2\kappa_3 - 5r^*\kappa_1^2\kappa_2 + 3r^*\kappa_1\kappa_2\kappa_3 + r^*\kappa_2^2\kappa_3 + \kappa_1^3 - 3\kappa_1^2\kappa_2 + \kappa_1^2\kappa_3 + \kappa_1\kappa_2\kappa_3\big]\big/(\kappa_1^2(\kappa_1 - \kappa_2)). \tag{11c}$$

The eigenvalues connected to the linear stability of the fixed point $N_{1,2,3} = 1$ are solutions of the equation

$$\lambda^3 + \lambda^2\kappa_1(1 + 3r^*) - \lambda[(\kappa_2\kappa_3 + 2\kappa_2^2 - \kappa_1^2)(1 + 6r^* + 9r^{*2})] - [(3\kappa_1\kappa_2^2 - \kappa_1^2\kappa_2 - \kappa_2^2\kappa_3 + \kappa_1\kappa_2\kappa_3)(1 + 9r^* + 27r^{*2} + 27r^{*3})] = 0 \tag{12}$$

for the case $\alpha^* = 0$.

The theorem of Shilnikov is satisfied in the parameter region where $\lambda_3 > 0$, $\lambda_{1,2} = \rho \pm \omega$ with negative real part ρ and imaginary ω. Finally we must have $\lambda_3 > -\rho$. In this paper we shall discuss the parameter region

$$\kappa_3 > \kappa_1 > \kappa_2 > 0 \tag{13}$$

that contains the parameters for the strange attractor discussed in [28].

Denoting $\delta = \kappa_2/\kappa_1 < 1$, $\theta = \kappa_3/\kappa_1 > 1$ and

$$C = 2r^*\delta^3 + (6r^* + 2)\delta^2 + (4r^* + 2)\delta \tag{14a}$$

$$D = 2r^*\delta^3 - (3r^* + 4)\delta^2 + (9r^* + 5)\delta - 2r^* - 1 \tag{14b}$$

we obtain that when $r^* > 0$ the area of validity of the Shilnikov theorem is where

$$0 < \delta < \frac{\sqrt{17} - 3}{4} \approx 0.2807 \tag{15}$$

and $\theta > 1$.

The area of validity for negative r^* is

$$-\frac{1}{2 + \delta} < r^* < 0 \tag{16}$$

and the restrictions on δ and θ are the same as (15) and

$$\theta > \max\left(1, -\frac{D}{C}\right). \tag{17}$$

Below we discuss the region of possible negative values of r^* as well as the region of positive values of r^* up to $r^* = 10$. Thus we investigate the case of small and medial adaptation of the growth rates of the populations.

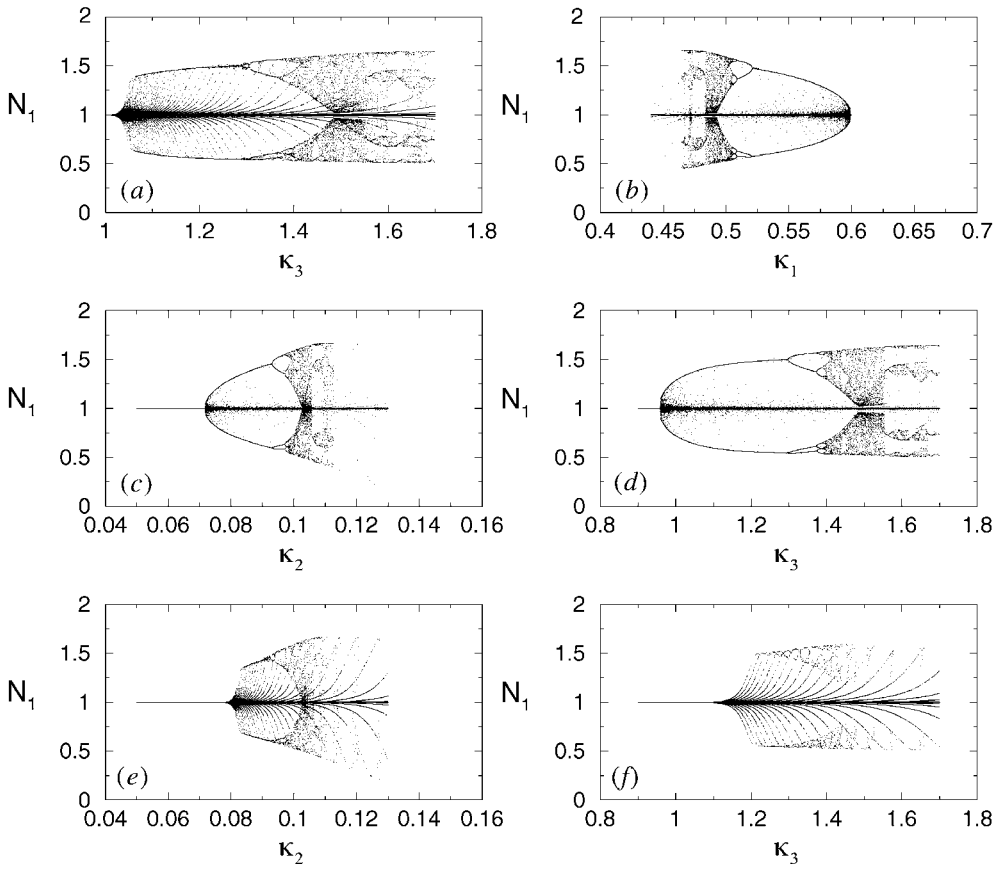

Figure 1. Bifurcation diagrams for N_1, obtained by a section of the attractor by means of a horizontal plane with coordinate equal to the z-coordinate of the fixed point P_2. (*a*) $r^* = 0$; $\kappa_1 = 0.5$; $\kappa_2 = 0.1$. (*b*) $r^* = 5$; $\kappa_2 = 0.1$; $\kappa_3 = 1.43$. (*c*) $r^* = 5$; $\kappa_1 = 0.5$; $\kappa_3 = 1.43$. (*d*) $r^* = 5$; $\kappa_1 = 0.5$; $\kappa_2 = 0.1$. (*e*) $r^* = -0.15$; $\kappa_1 = 0.5$; $\kappa_3 = 1.43$. (*f*) $r^* = -0.19$, $\kappa_1 = 0.5$; $\kappa_2 = 0.1$.

3. Attractors, power spectra, histograms and autocorrelations

Figure 1 shows bifurcation diagrams connected to the fixed point P_2. The starting point for the calculated trajectories is (0.999, 0.999, 0.999) i.e. in the vicinity of the fixed point P_2. The plots are obtained by fixing the number of individuals N_3 to the coordinate N_3^* of the fixed point P_2. By means of the plane defined in such a way a section of the attractor is obtained. Sequences of period-doubling and period-halving bifurcations as well as regions of dominant periodic and chaotic motions can be identified in figures 1(*a*)–(*f*). We note that the positive r^* change the shape of the Hopf bifurcation. This can be seen by a comparison of (*a*) and (*d*) of figure 1. The bifurcation diagrams from $r^* = 5$ to 10 have almost the same shape as the bifurcation diagrams for $r^* = 5$. The influence of r^* on the system attractor, when all the other parameters are fixed, can be seen in figure 2. Plot (*a*) shows that when r^* has an appropriate negative value the trajectory ends in a fixed point after some transition time. When $r^* = 0$ the attractor is a chaotic one and the increasing of r^* leads to a transformation of the attractor to a periodic one. We note that in figure 2(*b*) the period-three orbit (which is stable for the values of

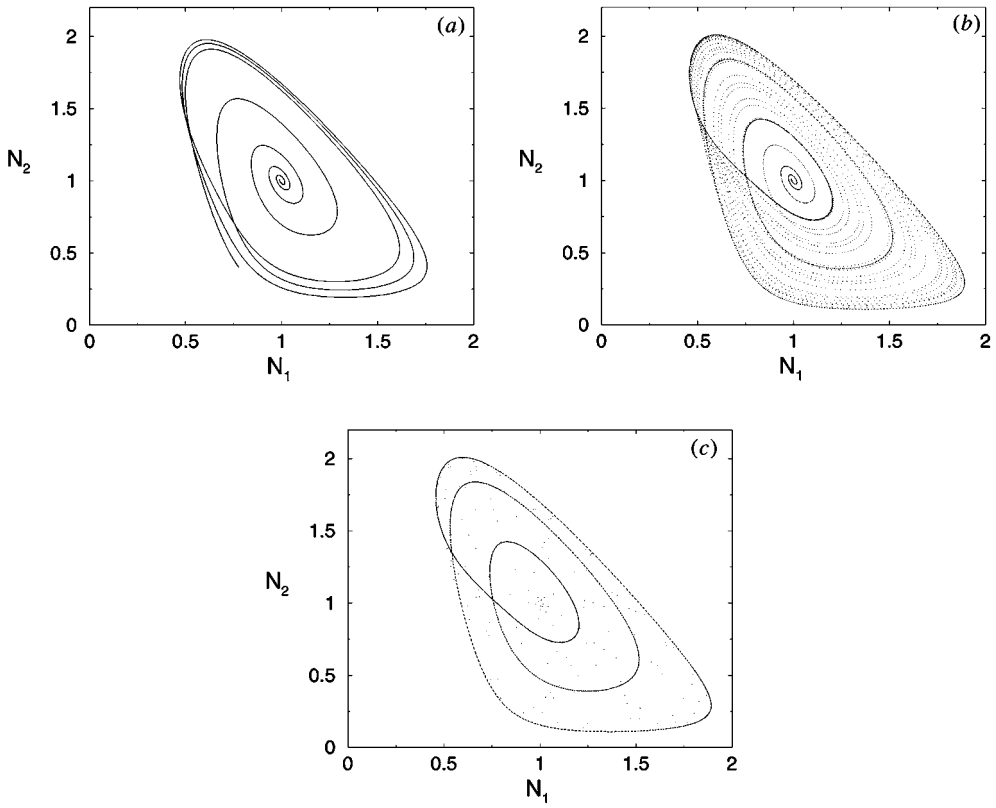

Figure 2. Influence of the parameter r^* on the attractor of the system. $\kappa_1 = 0.5$, $\kappa_2 = 0.1006$, $\kappa_3 = 1.43$. (*a*) $r^* = -0.2$. (*b*) $r^* = 0$. (*c*) $r^* = 5$.

the parameters corresponding to figure 2(*c*) is clearly visible despite the fact that the attractor is a chaotic one. The decreasing of r^* leads to a shift of the borders of the chaotic regions and the borders of the periodic windows. In addition the number of windows of periodic motion decreases with decreasing r^*.

Figure 3 presents the histograms for the number of individuals N_1 of the first population. The investigated time series consist of values sampled at equal time intervals. Thus the value of ρ^* shown in the figures is proportional to the time spent in some small interval around this quantity value. When a periodic motion is present the histograms exhibit two peaks per periodic component. These peaks correspond to the minimum and maximum number of individuals for the corresponding component of the periodic motion. Because of these features the histograms are the best tool for identifying the multiperiodic motions. The histograms in figure 3(*a*), (*b*) and (*d*) show clearly the presence of period-three cycles for the corresponding regions of system parameters.

Autocorrelations presented in figure 4 give information about the time evolution of the system. The autocorrelation A^* at lag l quantifies the distribution of the corresponding time series points p_k and p_{k+l}, $k = 1, 2, 3, \ldots$. If these points are evenly distributed in the plane (p_k, p_{k+l}) the autocorrelation is zero and a non-negative autocorrelation reflects a tendency of proportionality of p_k and p_{k+l} to each other. The autocorrelation for a periodic signal is also periodic and for deterministic chaotic systems the autocorrelation decays exponentially

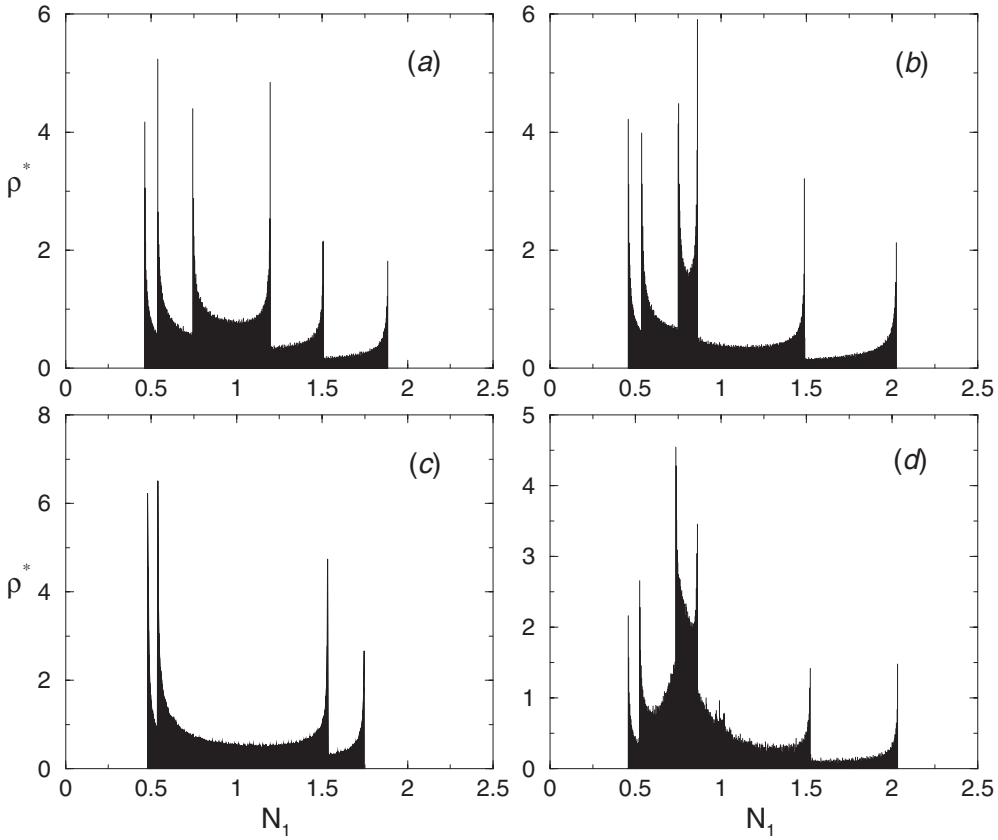

Figure 3. Histograms for the time series N_1 for the following values of the parameters. (a) $\kappa_1 = 0.5$; $\kappa_2 = 0.1$; $\kappa_3 = 1.443$; $r^* = 5$. (b) $\kappa_1 = 0.5$; $\kappa_2 = 0.1$; $\kappa_3 = 1.5545$; $r^* = 5$. (c) $\kappa_1 = 0.5$; $\kappa_2 = 0.1$; $\kappa_3 = 1.33$; $r^* = 5$. (d) $\kappa_1 = 0.5$; $\kappa_2 = 0.1$; $\kappa_3 = 1.56$; $r^* = -0.15$.

with increasing lag. The first zero of the autocorrelation function can be used as a time delay when we perform a time-delay reconstruction of the system dynamics from measured time series [32]. Figure 4(a) shows that the system dynamics is chaotic in the vicinity of the corresponding system parameters; (b)–(d) correspond to periodic motions.

The power spectral density (power spectrum)

$$S^*(f) = |H(f)|^2 + |H(-f)|^2 \qquad 0 \leqslant f \leqslant \infty \tag{18}$$

($H(f)$ is the function obtained by a Fourier transform of the investigated signal $h(t)$) visualizes the dominant frequencies connected to the system dynamics and their shifting when the system parameters change. If we use discrete sampled data with time interval Δ between the consecutive samples there exists a Nyquist critical frequency $f_c = 1/(2\Delta)$ (or $f_c = 1/2$ if we measure the time in units Δ). For the time series discussed here it is appropriate to use the power spectrum defined from 0 to f_c [33].

The chaotic motion is associated with the band part of the spectrum. In figure 5 power spectra are presented for several cases of system parameters: (b) and (c) show that the chaoticity of the attractor decreases with decreasing r^*. When r^* is negative the power spectral density is concentrated in the low-frequency area. With increasing r^* the power spectral density of the higher frequencies increases too. Figure 6 shows a typical picture of the changes in the

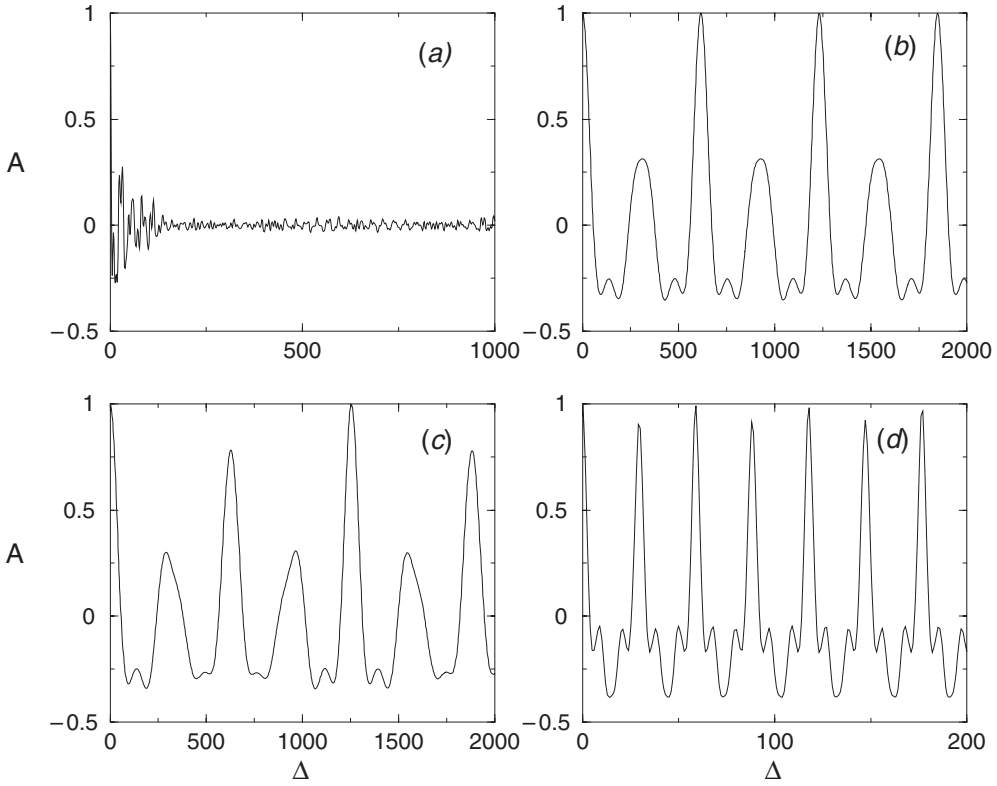

Figure 4. Autocorrelations for the time series for the following values of the variables. (*a*) $\kappa_1 = 0.467; \kappa_2 = 0.1; \kappa_3 = 1.43; r^* = 5$. (*b*) $\kappa_1 = 0.5; \kappa_2 = 0.1; \kappa_3 = 1.56; r^* = -0.15$. (*c*) $\kappa_1 = 0.5; \kappa_2 = 0.1; \kappa_3 = 1.57; r^* = -0.15$. (*d*) $\kappa_1 = 0.5; \kappa_2 = 0.1; \kappa_3 = 1.69; r^* = 5$. One unit for Δ corresponds to 20 integration steps.

attractor with increasing κ_3 in the presence of adaptation. The changes in the system dynamics with increasing control parameters κ_1 and κ_2 are presented in table 1.

4. Lyapunov exponents and Lyapunov dimension

The maximum Lyapunov exponent shows the following kind of motion in phase space: if $\lambda_{\max}$ is zero the motion is a stable limit cycle and for the chaotic motions $0 < \lambda_{\max} < \infty$. We compute $\lambda_{\max}$ by means of the sum [34, 35]

$$S(m, \epsilon, \delta t) = \frac{1}{N} \sum_{n_0=1}^{N} \ln \left[\frac{1}{X_{n_0}} \sum_{s \in X_{n_0}} |s_{n_0+\Delta n} - s_{n+\Delta n}| \right] \tag{19}$$

where in the embedding space X_{n_0} is the neighbourhood of diameter ϵ of the point s_{n_0} and δt is the time span. The sum over n_0 is used in order to average out the fluctuations of the expansion rates. S depends on the embedding dimension and on the size of the neighbourhood. When S has a linear increase with identical slope for all embedding dimensions larger than some m_0, and for large enough values of ϵ, then this slope is an estimation of the maximum Lyapunov exponent. Figure 7 shows several plots of the sum S. The slope of S is positive,

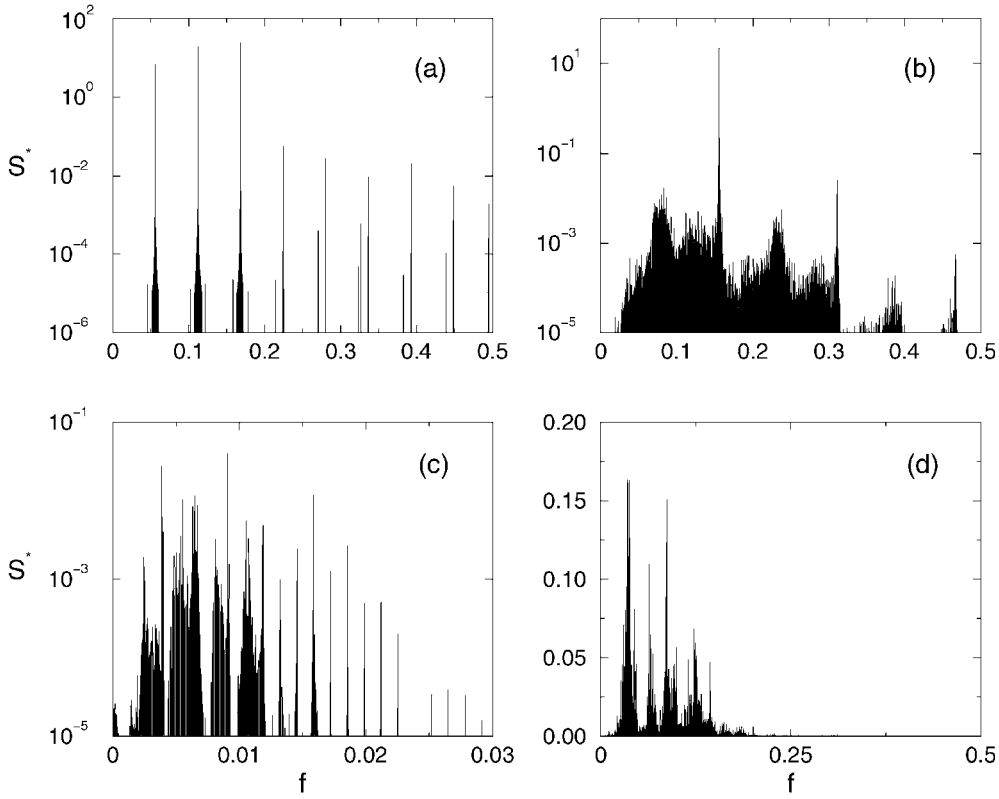

Figure 5. Power spectra for the time series N_1 for the following values of the parameters. (*a*) $\kappa_1 = 0.5$; $\kappa_2 = 0.1$; $\kappa_3 = 1.5545$; $r^* = 5$. (*b*) $\kappa_1 = 0.5$; $\kappa_2 = 0.1$; $\kappa_3 = 1.42$; $r^* = 5$. (*c*) $\kappa_1 = 0.5$; $\kappa_2 = 0.1$; $\kappa_3 = 1.43$; $r^* = -0.15$. (*d*) $\kappa_1 = 0.467$; $\kappa_2 = 0.1$; $\kappa_3 = 1.43$; $r^* = 5$.

which is an indicator for chaotic motion in these cases. We note that the maximum Lyapunov exponents for figures 7(*d*) and (*e*) are $\lambda_{\max} = 0.337 \pm 0.040$ and 0.345 ± 0.041 respectively. These values are close to the values obtained by the calculation of the Lyapunov spectrum as a function of $N\delta t$ (N, number of attractor points; δt, step of the numerical integration of the system of ODEs) [36] (figure 8(*a*), curves marked with diamonds and triangles). We note that the increase of κ_3 in the interval of values around 1.43 leads to a considerable increase of L_1 as well as to a smaller increase of the Lyapunov dimension (see figure 8(*d*)).

As we investigate a flow, one of the Lyapunov exponents must be zero. Indeed L_2 in figure 8(*b*) shows a tendency to reach zero with increasing N. The third Lyapunov exponent L_3 depends strongly on r^*: the decrease of R^* leads to an increase of L_3. Figure 8(*d*) shows the Lyapunov dimension [37]

$$D_{\mathrm{L}} = k + \frac{\sum_{i=1}^{k} \lambda_i}{|\lambda_{k+1}|}. \tag{20}$$

k is the maximum integer such that the sum of the k largest exponents is still non-negative. D_{L} is conjectured to coincide with the information dimension. The values of D_{L} for the four time series are slightly above two.

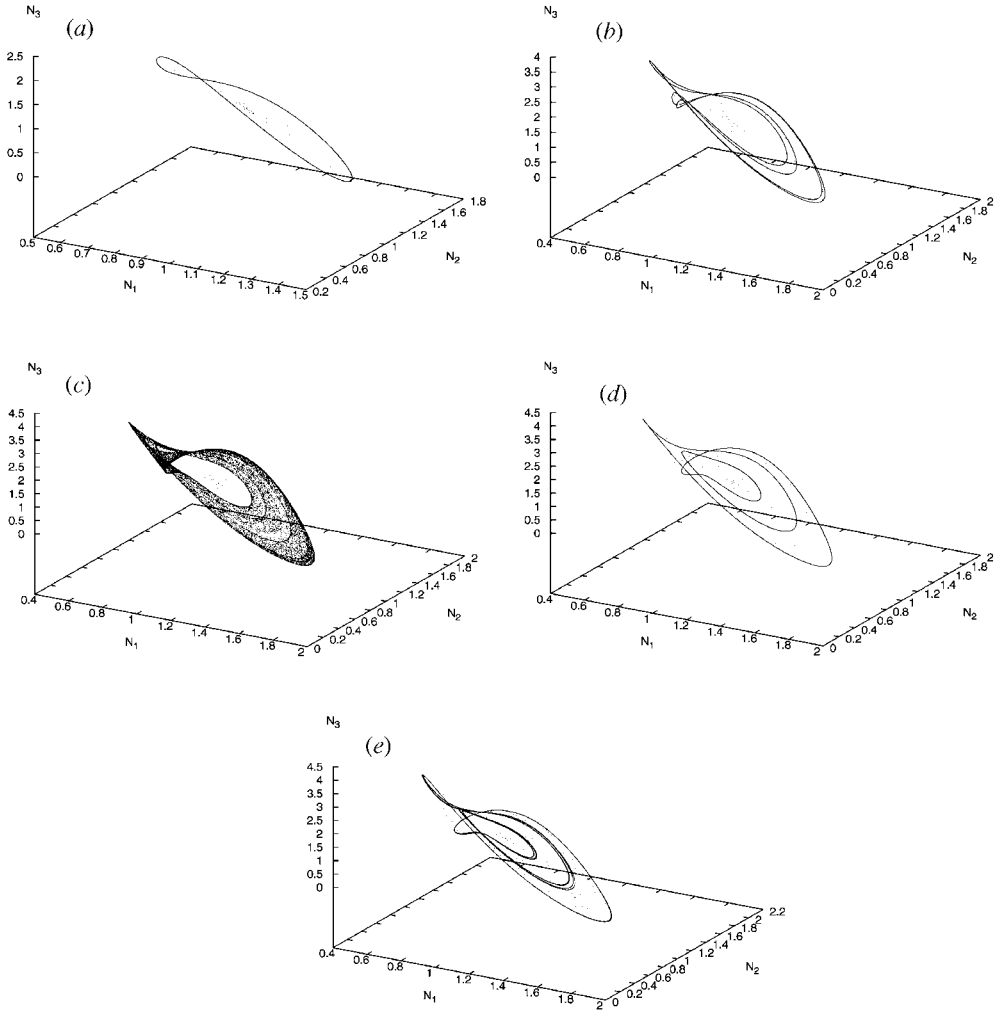

Figure 6. Attractors for the case $\alpha^* = 1.0$, $\kappa_1 = 0.5$, $\kappa_2 = 0.1$, $r^* = 5$. The values of κ_3 are as follows: (*a*) $\kappa_3 = 1.1$; (*b*) $\kappa_3 = 1.38$; (*c*) $\kappa_3 = 1.41$; (*d*) $\kappa_3 = 1.443$; (*e*) $\kappa_3 = 1.447$; (*f*) $\kappa_3 = 1.52$; (*g*) $\kappa_3 = 1.57$; (*h*) $\kappa_3 = 1.62$; (*i*) $\kappa_3 = 1.68$. (Continued opposite.)

5. Discussion

In this paper we have investigated the influence of an adaptation of the growth rates on the dynamics of the system of three populations competing for the same limited resource for the simplest case where the growth rate adaptation factors have small values and are the same for the three populations, and for parameter regions where the theorem of Shilnikov is satisfied. The adaptation influences the borders of the above-mentioned regions as well as leading to changes of the system dynamics. These changes increase with increasing r^*. When $\kappa_{1,2,3}$ are fixed and we change r^* there are regions where unstable periodic orbits can become stable. These orbits do not depend on the changes in r^* i.e., when a period-three orbit becomes stable it is always the same period-three orbit. In such cases the studied system shows insensitivity to the adaptation of the growth ratios of the populations. The

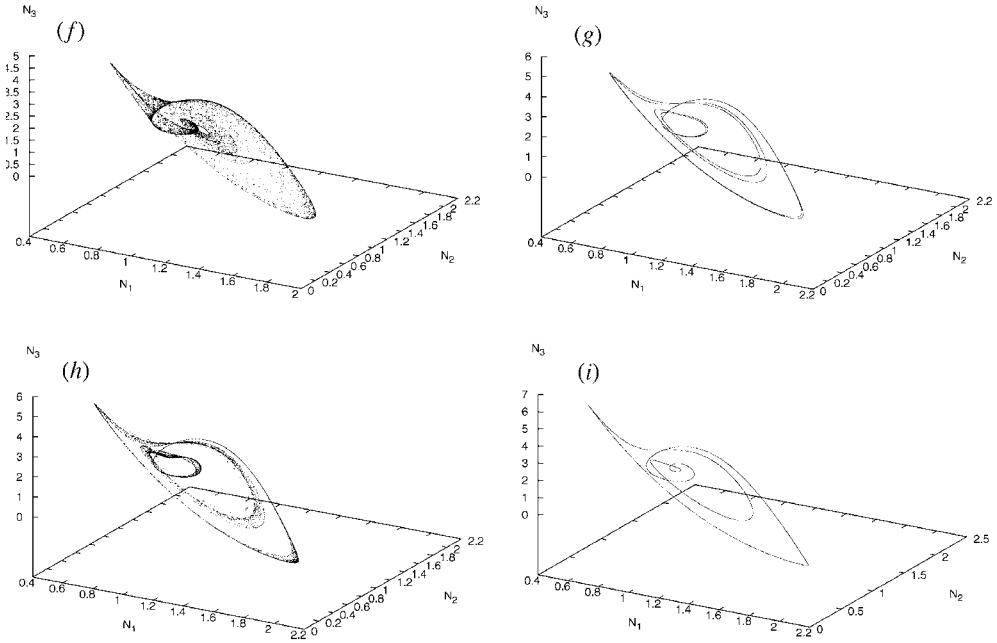

Figure 6. (Continued.)

changes of the value of r^* lead to changes of the profile of the Hopf bifurcation and the spectrum of the Lyapunov exponents is influenced too (especially the smallest Lyapunov exponent).

The investigated system exhibits the phenomenon of pairwise competition (species 1 beats species 2, species 2 beats species 3 and species 3 beats species 1) that is of interest not only for population dynamics but also in social sciences in connection to the theory of voting, where one quite often can see a cycling preference behaviour of the voters. Figure 9 shows that this phenomenon is present not only for the case of the periodic solutions of the model equations but also in the case of chaotic behaviour of the number of individuals. As a consequence of the pairwise competition the time is separated into intervals of domination of one of the populations and transition intervals where a shifting of the dominance to another population can be seen. We note that for the case discussed in this paper, population 2 has a negative growth rate $r_2^0 = -0.5$ while the growth rates of the other two populations are positive. Nevertheless due to the adaptation population 2 manages to be dominant, i.e. to have the highest number of individuals, in some time intervals. Thus the adaptation can be successful in compensating the negative consequences of a smaller growth ratio of a population. We note also that there exist differences in the pairwise competition behaviour for the case of a periodic solution of the model system of ODEs without competition and the pairwise competition behaviour for the case of chaotic solution of the model system of ODEs in the presence of adaptation of the growth rates. In the former case the transition periods are relatively small in comparison with the periods of a dominance of one of the populations, and the number of individuals of non-dominant populations is almost zero. In the chaotic case the transition periods are longer and the numbers of individuals of some of the non-dominant populations can be significantly different from zero.

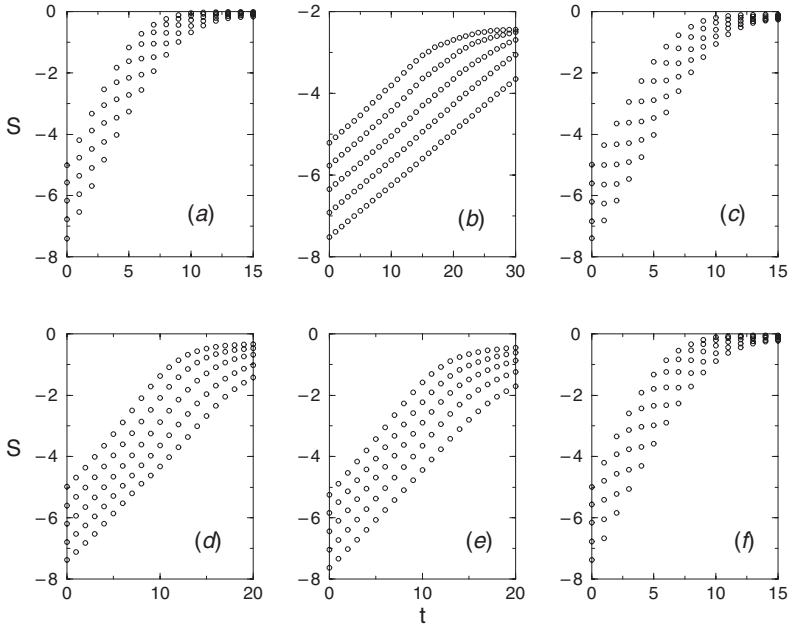

Figure 7. The sums S used for calculation of the maximum Lyapunov exponent. (a) $\kappa_1 = 0.48$; $\kappa_2 = 0.1$; $\kappa_3 = 1.43$; $r^* = 5$. (b) $\kappa_1 = 0.48$; $\kappa_2 = 0.1$; $\kappa_3 = 1.43$; $r^* = -0.15$. (c) $\kappa_1 = 0.5$; $\kappa_2 = 0.105$; $\kappa_3 = 1.43$; $r^* = 5$. (d) $\kappa_1 = 0.5$; $\kappa_2 = 0.1$; $\kappa_3 = 1.43$; $r^* = 5$. (e) $\kappa_1 = 0.5$; $\kappa_2 = 0.1$; $\kappa_3 = 1.43$; $r^* = -0.15$. (f) $\kappa_1 = 0.5$; $\kappa_2 = 0.1$; $\kappa_3 = 1.58$; $r^* = 5$.

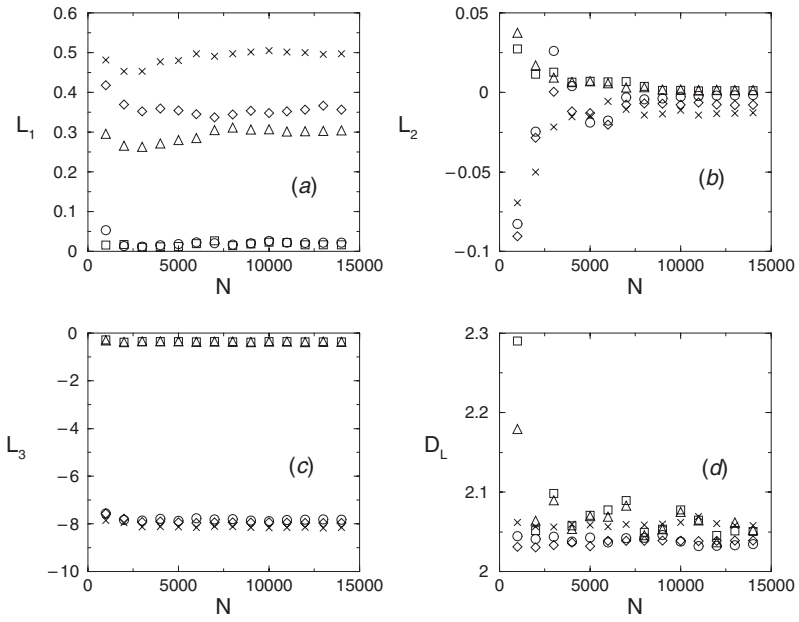

Figure 8. Lyapunov exponents $L_{1,2,3}$ and the Lyapunov dimension D_{L}. The different cases for the parameters are marked with the same symbols on each panel. The symbols are as follows: circles, $r^* = 5$, $\kappa_1 = 0.5$, $\kappa_2 = 0.1005$, $\kappa_3 = 1.43$; squares, $r^* = -0.1$, $\kappa_1 = 0.5$, $\kappa_2 = 0.1005$, $\kappa_3 = 1.43$; diamonds, $r^* = 5$, $\kappa_1 = 0.5$, $\kappa_2 = 0.1$, $\kappa_3 = 1.43$; triangles, $r^* = -0.1$, $\kappa_1 = 0.5$, $\kappa_2 = 0.1$, $\kappa_3 = 1.43$; x–s, $r^* = 5$, $\kappa_1 = 0.5$, $\kappa_2 = 0.1$, $\kappa_3 = 1.5$.

Table 1. Attracting manifolds for different control parameters.

$\kappa_1 = 0.5, \kappa_3 = 1.43$ $r^* = 5$	$\kappa_2 = 0.1, \kappa_3 = 1.43$ $r^* = 5$
κ_2	κ_1
$\leqslant$0.0716 Fixed point P_2	$\leqslant$0.46 Fixed point P_2
0.0716 Hopf bifurcation	0.46–0.467 Transient chaos
0.0716–0.0978 Transition to chaos by period-doubling bifurcations	0.467–0.505 Chaotic motion
0.0978–0.1058 Chaotic motion	0.505–0.599 Transition to a fixed point by period-halving bifurcations
0.1059 Period-three cycle	$>$0.599 Fixed point
0.1059–0.106 Transition to chaos by period-doubling bifurcations	
0.106–0.114 Chaotic motion	
$>$0.114 Fixed point, a small region of transient chaos exists	

The value of the Lyapunov dimension remains around two in the investigated parameter intervals. Therefore, if the investigated system has appropriate dissipation properties it may be eligible for a topological analysis. In order to investigate these properties we denote the right-hand side of the system of equations (6) as $\boldsymbol{F} = (F_1, F_2, F_3)$ with

$$F_i = N_i \sum_{j=1}^{n} \kappa_{ij}(1 - N_j) + A_i. \tag{21}$$

The divergence of $\boldsymbol{F}$ is equal to the sum of the local Lyapunov exponents [38, 39] and if $\mathrm{div}\boldsymbol{F}$ is negative everywhere the corresponding system is dissipative. We have to calculate $\mathrm{div}\boldsymbol{F}$ in local coordinates around a point $(N_{1,0}, N_{2,0}, N_{3,0})$. Neglecting all terms in the Taylor series for the divergence of $\boldsymbol{F}$ containing the local coordinates and when the remaining term is not very small

$$\mathrm{div}\boldsymbol{F} \approx \mathrm{Tr}\left[\left(\frac{\partial F_i}{\partial N_j}\right)\Big|_{(N_{1,0}, N_{2,0}, N_{3,0})}\right]. \tag{22}$$

For some systems of ODEs (22) does not depend on the coordinates $N_{i,0}$ (an example is the system leading to the famous Lorentz attractor). This is not the case for the system studied here. We obtain

$$\mathrm{div}\boldsymbol{F} \approx \kappa_1[1 - N_{1,0} - N_{2,0}] + \kappa_2[3 + N_{2,0} - 4N_{3,0}] + \kappa_3[1 - N_{1,0}] = I_1 \tag{23}$$

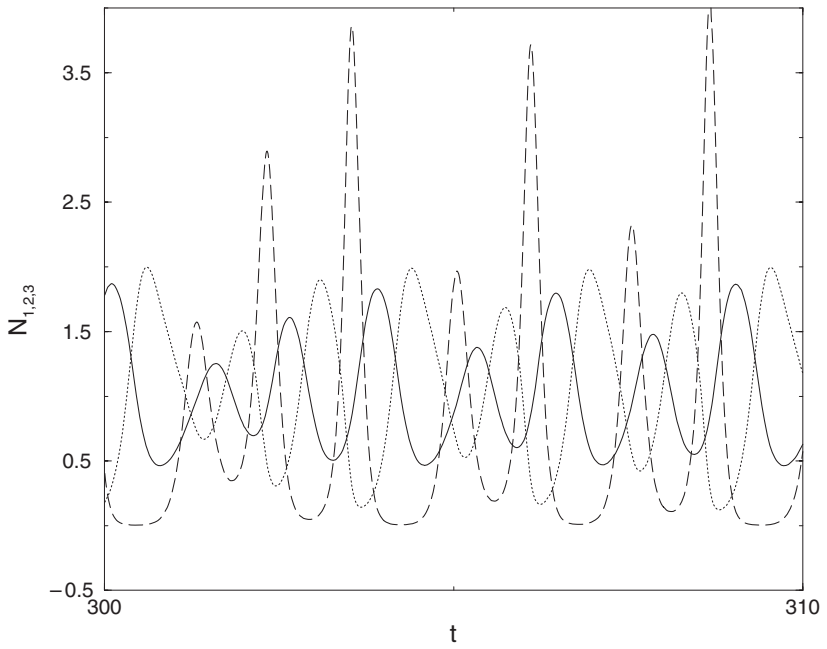

Figure 9. Pairwise competition among the populations. Solid curve: N_1. Dotted curve: N_2. Dashed curve: N_3. $\kappa_1 = 0.5$; $\kappa_2 = 0.1$; $\kappa_3 = 1.43$; $r^* = 5$.

for the case without adaptation and

$$\mathrm{div}\boldsymbol{F} \approx I_1 + r^*\Bigg[\sum_{i=1}^{3} r_i^0 N_{i,0} + \sum_{i,j=1}^{3} r_i^0 N_{j,0} - \sum_{i,j,l=1}^{3} r_i^0 \alpha_{ij}^0 N_{j,0} N_{l,0} - \sum_{i,l=1}^{3} r_i^0 \alpha_{ii}^0 N_{i,0} N_{l,0} - \sum_{i,j=1}^{3} r_i^0 \alpha_{ij}^0 N_{i,0} N_{j,0}\Bigg] \tag{24}$$

for the case with adaptation and $\alpha^* = 0$. Negative values of r^* lead to positive $\mathrm{div}\boldsymbol{F}$ and thus to a worsening of the dissipative properties of the system. Positive values of r^* lead to negative values of $\mathrm{div}\boldsymbol{F}$. Thus the increasing adaptation of the population growth rates lead to decreasing of the dimension of the chaotic attractors (the attractors become thinner). In addition to this the largest Lyapunov exponents have small positive values in comparison with the corresponding absolute values of the smallest Lyapunov exponents. These features of the case of positive r^* make the attractors of the investigated system eligible for analysis of their topological properties, and for calculation of topological invariants such as linking and rotation numbers [39]. This analysis will be a subject of future research.

Acknowledgments

We thank H Kantz, R Hegger and T Schreiber for the stimulating discussions and useful comments in connection with the calculation of the Lyapunov exponents and using the TISEAN software package [40].

References

[1] May R M 1975 *J. Theor. Biol.* **51** 511
[2] May R M 1976 *Am. Naturalist* **110** 573
[3] May R M 1976 *Nature* **261** 459
[4] May R M 1976 *Theor. Popul. Biol.* **9** 178
[5] Ives A R and May R M 1985 *J. Theor. Biol.* **115** 65
[6] May R M 1987 *Proc. R. Soc.* A **413** 27
[7] Sugihara G and May R M 1990 *Nature* **344** 734
[8] Sugihara G and May R M 1990 *Trends Ecol. Evol.* **5** 79
[9] Hassel M D, Comins H N and May R M 1991 *Nature* **353** 255
[10] Nee S and May R M 1992 *J. Anim. Ecol.* **61** 37
[11] Lloyd A L and May R M 1999 *Trends Ecol. Evol.* **14** 417
[12] Volterra V 1931 *Leçons sur la Théory Mathématique de la Lutte pour la Vie* (Paris: Gouttiers-Vallard)
[13] Lotka A J 1956 *Elements of Mathematical Biology* (New York: Dover)
[14] Ayala F J, Gilpin M J and Ehrenfield J G 1973 *Theor. Popul. Biol.* **4** 331
[15] Jorné J 1975 *J. Theor. Biol.* **65** 133
[16] May R M and Leonard W J 1975 *SIAM J. Appl. Math.* **29** 243
[17] Satulovsky J E 1996 *J. Theor. Biol.* **183** 381
[18] Begon M, Harper J L and Towsend C R 1990 *Ecology: Individuals, Populations and Communities* (Boston, MA: Blackwell)
[19] Murray J D 1993 *Mathematical Biology* (Berlin: Springer)
[20] Johnson T and Ebenman B 1998 *J. Theor. Biol.* **193** 407
[21] Vereecken K M, Dens E J and Van Impe F F 2000 *J. Theor. Biol.* **205** 53–72
Vereecken K M, Dens E J and Van Impe F F 2000 *J. Stat. Phys.* **27** 171–82
[22] Dimitrova Z I and Vitanov N K 2000 *Phys. Lett.* A **272** 368
[23] Gilpin M E 1979 *Am. Naturalist* **113** 306
[24] Klebanoff A and Hastings A 1994 *Math. Biosci.* **122** 221
[25] Schnabl W, Stadler P F, Forst C and Schuster P 1991 *Physica* D **48** 65
[26] Hastings A and Powell T 1991 *Ecology* **72** 896
[27] Klebanoff A and Hastings A 1994 *J. Math. Biol.* **32** 427
[28] Arneodo A, Coullet P and Tresser C 1980 *Phys. Lett.* A **79** 259
[29] Shilnikov L P 1965 *Sov. Math.–Dokl.* **6** 163
[30] Arneodo A, Coullet P and Tresser C 1982 *J. Stat. Phys.* **27** 171
[31] Kuznetsov Y A 1995 *Elements of Applied Bifurcation Theory* (Berlin: Springer)
[32] Abarbanel H D I 1996 *Analysis of Chaotic Time Series* (Berlin: Springer)
[33] Press W H, Teukolsky S A, Vetterling W T and Flannery B P 1997 *Numerical Recipes in C, the Art of Scientific Computing* (Cambridge: Cambridge University Press)
[34] Kantz H 1994 *Phys. Lett.* A **185** 77
[35] Rosenstein M T, Colins J J and de Luca C J 1993 *Physica* D **65** 117
[36] Nusse H E and Yorke J A 1994 *Dynamics: Numerical Explorations* (Berlin: Springer)
[37] Frederickson P, Kaplan J L, Yorke E D and Yorke J A 1983 *J. Diff. Eqns* **49** 185
[38] Gilmore R 1993 *Catastrophe Theory for Scientists and Engineers* (New York: Dover)
[39] Gilmore R 1998 *Rev. Mod. Phys.* **70** 1455
[40] Hegger R, Kantz H and Schreiber T 1999 *Chaos* **9** 413